CAMDA: Capacity Assessment Method for Decentralized Air Traffic Control

Sunil, Emmanuel; Ellerbroek, Joost; Hoekstra, Jacco

Publication date
2018

Document Version
Accepted author manuscript

Published in
2018 International Conference on Research in Air Transportation

CAMDA: Capacity Assessment Method for Decentralized Air Traffic Control

Emmanuel Sunil, Joost Ellerbroek and Jacco M. Hoekstra
Faculty of Aerospace Engineering, Delft University of Technology
Kluyverweg 1, 2629 HS, Delft, The Netherlands

***Abstract*—This paper presents a semi-empirical method to determine the maximum theoretical capacity of decentralized airspace concepts. The method considered here, named Capacity Assessment Method for Decentralized ATC (CAMDA), formalizes an earlier approach described in literature, extends it for three-dimensional airspace, and also improves the accuracy of the underlying models. CAMDA defines capacity as the traffic density at which conflict chain reactions propagate uncontrollably throughout the entire airspace. CAMDA identifies this critical density using a semi-empirical approach whereby models describing the actions of decentralized conflict detection and resolution algorithms are combined with empirically obtained conflict count data. The CAMDA method is demonstrated in this work for a decentralized direct routing en-route airspace concept that utilizes a state-based conflict detection algorithm, and a voltage potential-based conflict resolution algorithm. Three fast-time simulation experiments were performed to study how the capacity of this particular airspace design is affected by: a) conflict detection parameters; b) conflict resolution dimension; and c) the speed distribution of aircraft. The results showed that CAMDA estimated the occurrence of conflict chain reactions with high accuracy for all cases, enabling capacity estimations using relatively non-intensive low density traffic simulations. Therefore, CAMDA can be used to speed up the airspace design process by reducing the number of time consuming high-density traffic simulations that are required when performing a trade-off between different airspace designs, or when fine-tuning the parameters of the selected airspace design.**

***Keywords*—Airspace capacity; airspace stability; Domino Effect Parameter (DEP); self-separation; BlueSky ATM simulator**

I. Introduction

Despite the significant R&D efforts undertaken to overhaul aging Air Traffic Control (ATC) systems, air traffic delays and congestion continue to rise at an alarming rate [1]. In response to this pressing issue, several researchers have long advocated for a transfer of traffic separation responsibilities in en-route airspace from ground-based Air Traffic Controllers (ATCos) to each individual aircraft [2]–[4]. The resulting decentralized traffic separation paradigm has been shown to increase airspace capacity over current centralized operations by increasing the efficiency with which the available airspace is utilized [2]–[4].

To support decentralization, the research community has largely focused on developing automated algorithms for airborne Conflict Detection and Resolution (CD&R) [5]. Some studies in this domain have also investigated if such algorithms can be combined with different options for structuring air traffic to further increase capacity over current operations [6].

However, in spite of over two decades of active research highlighting its theorized benefits, as well as successful flight-test demonstrations over Mediterranean airspace [7], decentralization is yet to be deployed in the field. From a technical point of view, one possible reason for the reluctance to introduce decentralization may be explained by an insufficient understanding of the factors that affect airspace capacity for decentralization. This aspect is further complicated by the fact that most capacity measurement tools, such as those related to ATCo workload, are not relevant for decentralized ATC.

But before a comprehensive capacity assessment method can be developed for decentralized ATC, it is first necessary to consider what the term 'airspace capacity' refers to in a more general sense. At a fundamental level, airspace capacity, regardless of the type or location of separation management, can be considered equivalent to the density at which the airspace becomes saturated; i.e., the density beyond which no additional traffic can be accommodated without significantly degrading system-wide macroscopic properties; properties such as the safety and efficiency of travel.

Using this view of airspace capacity as a starting point, previous research has identified airspace stability, which considers the propagation of conflicts as a result of tactical Conflict Resolution (CR) maneuvers, as an important aspect when evaluating the saturation density of decentralized ATC [8], [9]. These studies have shown that CR can destabilize the airspace at high traffic densities by triggering *conflict chain reactions* due to the scarcity of airspace, as well as due to the type of airspace design and CD&R algorithms used. To measure airspace stability, literature has also presented the so called Domino Effect Parameter (DEP) metric [8], [9]. The DEP was subsequently used by Jardin to relate airspace stability to capacity for decentralization [10]. While Jardin's approach provides an innovative method for measuring airspace capacity, it is only applicable for motion restricted to the horizontal plane. Therefore the method, as derived by Jardin, does not account for the effect of climbing/descending traffic, or the effect of cruise-climb procedures, on capacity.

The main goal of the current paper is to extend Jardin's method for application in three-dimensional airspace such that the effects of all flight phases on capacity can be taken into account. Additionally, we have used our past experiences in developing and validating conflict count models to further increase the realism and accuracy of the method [11], [12]. The resulting improved method, termed here Capacity Assessment Method for Decentralized ATC (CAMDA), makes use of the DEP to define the maximum theoretical capacity of decentralized airspace as the density at which conflict chain reactions become uncontrollable. Because conflict chain reactions are caused by many interconnected factors that cannot be accurately modeled for all conditions in a purely analytical sense, CAMDA is a semi-empirical approach. Therefore CAMDA relies on empirical data, obtained through simulation, to apply its capacity definition, and evaluate the capacity of a particular airspace concept. Nonetheless, because the underlying CAMDA models are based on the processes that govern CD&R, all its parameters have physical meaning. As such, the structure of the CAMDA models themselves provide useful insights into the relationships between the factors that affect capacity for decentralization.

This paper begins with an overview of the relevant definitions in section II. Next, in section III, the complete derivation of the CAMDA method is presented. To illustrate the utility of the developed method, it is applied on empirical data gathered from fast-time simulations of a direct-routing en-route airspace concept that utilizes a state-based Conflict Detection (CD) algorithm, and a voltage potential-based CR algorithm. The design of these simulation experiments, which consider the effects of CD parameters, CR dimension, and the speed distribution of aircraft on capacity, are described in section IV. The results of the CAMDA method for the considered airspace design are given in section V. Finally, the main conclusions of this study are summarized in section VI.

II. Background

This section summarizes the definitions and background material used by the CAMDA method.

A. The Difference Between Conflicts and Intrusions

A conflict occurs if the horizontal and vertical distances between two aircraft are expected to be less the prescribed separation standards within a predetermined 'look-ahead' time. Conflicts are, therefore, predictions of *future* separation violations. Intrusions, also referred to as losses of separation, occur when separation requirements are violated at the *present* time. This distinction between conflicts and intrusions is shown in Fig. 1.

As mentioned earlier, CAMDA is concerned with the occurrences of conflict chain reactions. Therefore, the rest of this paper only deals with aspects that are relevant to conflicts.

B. Airspace Stability and the Domino Effect Parameter

Airspace stability relates to the occurrence of conflict chains when tactical CR maneuvers are used. At high traffic densities, such chain reactions can 'destabilize' the airspace by propagating conflicts throughout the entire airspace. To measure the propagation of conflict chain reactions, literature introduces the 'Domino Effect Parameter' (DEP) [8], [9]. The DEP can be visualized using the Venn diagram in Fig. 2. Here, $C_{total,nr}$ is the set of all conflicts without CR, and $C_{total,wr}$ is the set of all conflicts with CR, for identical traffic scenarios. Furthermore, three regions can be identified in Fig. 2; $R1$, $R2$ and $R3$. By comparing $R3$ with $R1$, the proportion of 'destabilizing' conflicts caused by CR can be determined. Thus, the DEP is defined as:

$$DEP = \frac{R3\,(\rho) - R1\,(\rho)}{C_{total,nr}\,(\rho)} = \frac{C_{total,wr}\,(\rho)}{C_{total,nr}\,(\rho)} - 1 \qquad (1)$$

The number of conflicts that occur is dependent on the traffic density, ρ, regardless of whether CR is used. Hence, all parameters in the above equation are a function of ρ.

To interpret the output of the above equation, it is useful to categorize conflicts in R_1, R_2, and R_3. First, conflicts that are common to both the CR OFF and CR ON cases are given by R_2. However, as soon as CR is applied, the aircraft that suffer conflicts will fly different routes, both spatially and temporally. Because of this, some conflict pairs that would have occurred with the original CR OFF trajectories will be avoided, and similarly, the altered CR ON trajectories can also trigger different conflict pairs. In Fig. 2, R_1 represents the avoided conflict pairs, and R_3 corresponds to the additional, different conflict pairs. These additional conflict pairs can be either due to chance, or due to chain reactions, where a conflict resolution of a *primary* conflict immediately triggers a *secondary*, or knock-on, conflict. Therefore it follows that the numerator, $R_3 - R_1$, indicates the amount by which the number of additional conflicts outweighs the number of conflicts that are avoided with CR, and as such, the net destabilizing effect of CR (or stabilizing if $R_1 > R_3$). If it is assumed that conflict probability doesn't change due to CR, the *number* of primary conflicts can be considered equivalent to $C_{total,nr}$, i.e., the

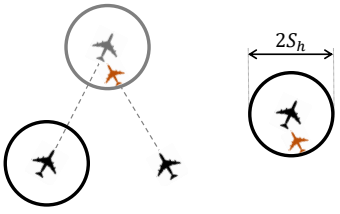

(a) Conflict (b) Intrusion

Fig. 1. The difference between intrusions and conflicts, displayed here for the horizontal plane. Here, S_h is the horizontal separation requirement.

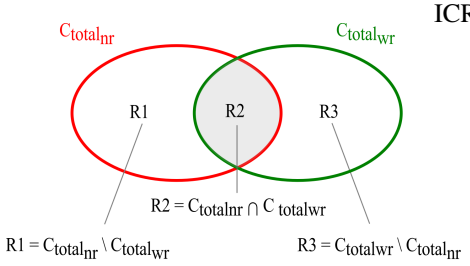

Fig. 2. The Domino Effect Parameter (DEP) compares simulations with and without Conflict Resolution (CR) to measure airspace stability

denominator of the above equation[1]. Consequently, based on the structure of (1), the DEP can be thought of as the *number of secondary conflicts per primary conflict*. Correspondingly, a higher value of DEP indicates higher airspace instability.

As the DEP is concerned with conflict chains, it is invariably linked to the safety of the airspace. But because conflict chain reactions also increase the flight distances of aircraft, the DEP, and consequently the notion of airspace airspace stability, also relates to airspace efficiency. The ability to simultaneously consider both the safety and efficiency of air travel makes the DEP a powerful tool for airspace capacity analysis purposes.

III. The CAMDA Method

This section presents the complete derivation of the CAMDA method. It begins by introducing the airspace capacity definition used by CAMDA. This definition is subsequently used to derive the six components of the CAMDA approach.

A. CAMDA Capacity Definition

When a conflict occurs, a conflict resolution action needs to be taken to prevent that conflict from turning into an intrusion. In the case of decentralized ATC, these resolutions can be determined by pilots, or by automated onboard CR algorithms. In either case, such tactical CR maneuvers can cause new conflicts, and in some cases, they can trigger conflict chain reactions. At low traffic densities, the ample maneuvering room available would, under normal conditions, allow such chain reactions to dissipate by themselves, i.e., without external intervention.

When extrapolating this logic for extreme traffic densities, it is likely that at a critical traffic density, the scarcity of airspace becomes so severe that conflict chain reactions propagate throughout the entire airspace. This would cause all aircraft to be inter-connected by a continuous, and perpetual conflict chain. Under such circumstances, it is unlikely that any CR maneuver by any aircraft could stabilize the airspace system. This would in turn result in an uncontrollable situation where all aircraft are resigned to continually perform meaningless CR maneuvers, without ever being able to fly to their actual destinations. The CAMDA method defines the maximum *theoretical* capacity of a decentralized airspace design at this critical traffic density.

To pin-point the aforementioned hypothetical density at which conflict chain reactions are uncontrollable, CAMDA makes use of the DEP; if all aircraft are 'stuck' in conflict at the maximum theoretical density, then an *infinite* number of secondary conflicts would be triggered by the resolution of any primary conflict. Therefore, *CAMDA defines the maximum theoretical capacity as the density at which the rate of change of the DEP with density tends to infinity.* More formally, the CAMDA capacity definition can be stated as:

$$\boxed{\lim_{\rho \to \rho_{max}} \frac{dDEP\,(\rho)}{d\rho} = \infty, \text{ where } \rho_{max} \equiv \text{capacity}} \qquad (2)$$

[1]CR maneuvers are unlikely to reduce the *number* of conflicts compared to the no resolution case, expect for relatively low traffic densities when CD&R algorithms are combined with Conflict Prevention (CP) systems. CP is not considered in this work. Refer to [2] for more on CP.

B. CAMDA Framework

To evaluate the CAMDA capacity definition given by (2), it is necessary to express the DEP as a function of ρ. As indicated by (1), this requires the derivation of models for $C_{total,nr}$ and $C_{total,wr}$ as functions of ρ. CAMDA derives such expressions using a six-step sequential framework, see Fig. 3. Here it can be seen that the framework consists of two main parts. The first part focuses on modeling $C_{total,nr}$, while the second focuses on modeling $C_{total,wr}$. Two assumptions, shown on the left side of Fig. 3, are used to bridge these two main parts of the framework. The final step uses these models, and applies the CAMDA capacity definition to determine ρ_{max} via the DEP.

Before proceeding with the derivation of the CAMDA model components, it is necessary to highlight three aspects.

Firstly, it should be noted that CAMDA is a semi-empirical method as one of its parameters need to be determined directly from simulation data. This is because conflict chain reactions, which are central to the CAMDA capacity definition, are dependent on a number inter-linked factors, and the effects of these interactions on capacity are difficult to model accurately using a purely analytical approach. These include emergent behavior that results from interactions between the considered CD&R algorithms and the selected mode for structuring air traffic.

Secondly, this work aims at demonstrating CAMDA for a three-dimensional direct-routing en-route airspace design that is combined with a state-based CD algorithm, and a voltage potential-based CR algorithm. Hence the models, as derived here, are only applicable for this particular case. Nevertheless, the basic framework displayed in Fig. 3 can be applied to any given decentralized airspace design. Because CAMDA is sequential, this mostly involves making appropriate modifications to the first step of the CAMDA framework.

Finally, it should be noted that CAMDA is inspired by Jardin [10]. In addition to formalizing Jardin's approach, the current paper extends his method for three-dimensional airspace. Furthermore, because CAMDA relies on a sequential framework, by using an improved model for the first step of the CAMDA framework using results from our prior work [11], [12], the accuracy and realism of all subsequent steps is also expected to be higher than in [10].

C. Step 1: Instantaneous Conflict Count Without CR

The goal of the first part of the CAMDA framework is to compute the total number of conflicts without CR: $C_{total,nr}$. As can be seen in Fig. 3, this process begins by modeling the instantaneous conflict count without CR, $C_{inst,nr}$, as a function of the number of instantaneous aircraft in the airspace without CR, $N_{inst,nr}$. $C_{inst,nr}$ will subsequently be used to calculate $C_{total,nr}$ in the next step of the derivation.

For any airspace design, $C_{inst,nr}$ can be modeled as the product of two factors, namely the number of combinations of two aircraft, and the conflict probability between any two aircraft, p. In essence, the number of combinations of two aircraft is the maximum number of conflicts that can occur, since multi-aircraft conflicts, i.e., conflicts involving more than two aircraft, can also be decomposed into a series of two-aircraft conflicts. The conflict probability, on the other hand, scales down the number of combinations so that only those aircraft that are within range each other and those with intersecting trajectories are counted as conflicts.

For the unstructured airspace design that is the focus of this derivation process, the number of combinations can be computed directly using the binomial theorem, since this airspace design imposes no constraints on the motion of aircraft [11], [12]. Therefore, $C_{inst,nr}$ can be expressed as:

$$C_{inst,nr} = \frac{N_{inst,nr}\left(N_{inst,nr}-1\right)}{2}\, p \tag{3}$$

To model the conflict probability, p, it is necessary to consider the process of CD. In state-based CD, aircraft search for conflicts within a volume of airspace in front of them. In essence, this involves a 4D extrapolation of aircraft position vectors, assuming constant velocity vectors. Therefore, p can be computed as the ratio between the volume of airspace searched for conflicts, B_c, and the total volume of the airspace under consideration, B_{total}. For mathematical convenience, B_c can be decomposed into its horizontal and vertical components, see Fig. 4. Using this approach, p as can be expressed as:

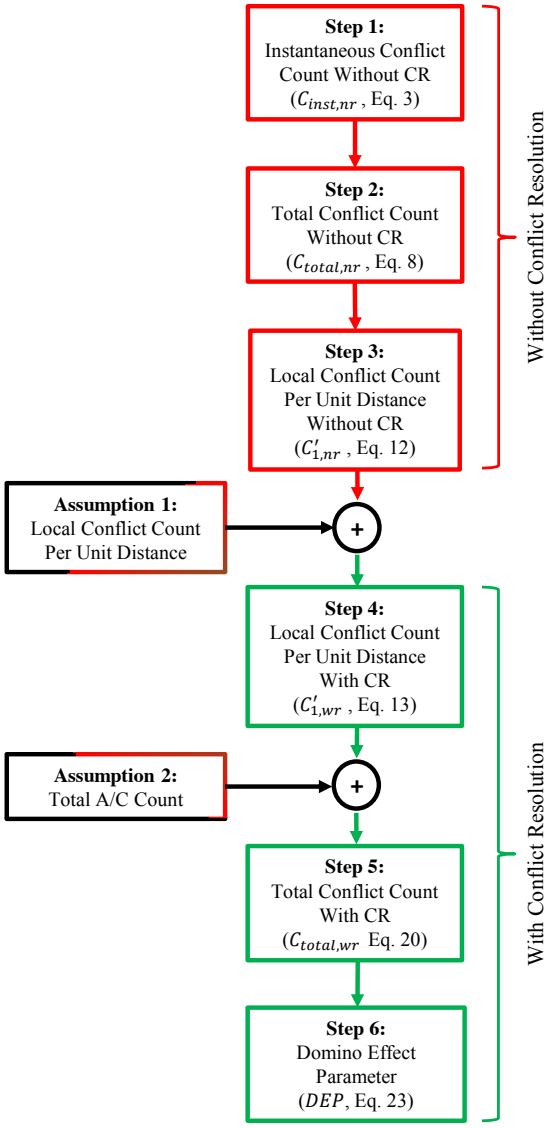

Fig. 3. Six steps of the CAMDA framework

$$p = \frac{B_{c,h}+B_{c,v}}{B_{total}} = \frac{4\ S_h S_v\ \mathbf{E}\left(V_{r,h}\right) t_l + \pi S_h^2\ \mathbf{E}\left(V_{r,v}\right) t_l}{B_{total}} \tag{4}$$

Here, S_h and S_v are the horizontal and vertical separation requirements, and t_l is the CD 'look-ahead' time. $\mathbf{E}\left(V_{r,h}\right)$ and $\mathbf{E}\left(V_{r,v}\right)$, are the horizontal and vertical components of the expected relative velocity of all aircraft pairs. The expected relative velocity can be considered equivalent to the weighted average of the relative velocity of all aircraft pairs in the airspace, taking into account the heading, altitude, spatial and speed distributions of all aircraft. For a direct-routing unstructured airspace design, we have derived the following expressions for these two variables in our prior work [12]:

$$\mathbf{E}\left(V_{r,h}\right) = \frac{4V}{\pi} \tag{5a}$$

$$\mathbf{E}\left(V_{r,v}\right) = V\sin\left(\gamma\right)\left(1-\varepsilon^2\right) \tag{5b}$$

Here, V is aircraft ground speed, γ is the flight path angle

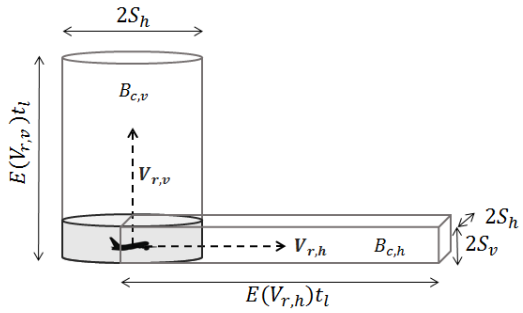

Fig. 4. Volume searched for conflicts by an aircraft in 3D airspace

of climbing/descending aircraft, and ε is the proportion of cruising aircraft in the airspace. All three variables are traffic scenario related. Furthermore, the specific version of (4) and (5) apply only for scenarios with uniform heading, altitude, and spatial distributions. The above equations also assume all aircraft to fly with equal ground speeds. Because CAMDA is a sequential method, these assumptions affect subsequent steps of the derivation. Nevertheless, the effect of the equal speed assumption on CAMDA is specifically tested in this research, see section V-C. The reader is referred to [13] for alternate versions of $\mathbf{E}(V_{r,h})$ and $\mathbf{E}(V_{r,v})$ for cases where the above 'ideal' traffic scenario assumptions do not hold.

D. Step 2: Total Conflict Count Without CR

The total number of conflicts without CR, $C_{total,nr}$, can be computed by summing up the number of instantaneous conflicts detected at each time step during an analysis time interval T. The result of this summation should be divided by the average conflict duration, t_c, so that conflicts which occur over multiple time steps are only counted once. Since a continuous summation over time is equivalent to an integration over time, a model for $C_{total,nr}$ can be computed as:

$$\begin{aligned} C_{total,nr} &= \frac{1}{t_c}\int_0^T C_{inst,nr}dT \\ &= \frac{C_{inst,nr}T}{t_c} \end{aligned} \tag{6}$$

To introduce traffic density, ρ, into the derivation process, the following relationship between the number of instantaneous aircraft, $N_{inst,nr}$, and the area of the airspace, A, can be used:

$$\rho = \frac{N_{inst,nr}}{A} \tag{7}$$

Substitution of (3) and (7) into (6) leads to the following final expression for $C_{total_{nr}}$:

$$C_{total,nr} = \frac{pTA^2\rho\left(\rho - \frac{1}{A}\right)}{2t_c} \approx \frac{pTA^2\rho^2}{2t_c} \quad \text{if } \rho \gg \frac{1}{A} \tag{8}$$

Note that the above equation has been simplified using the fact that $\rho - 1/A \approx \rho$ for practical values of ρ and A. Also note that under ideal conditions, t_c is equal to the look-ahead time, t_l, for state-based CD. However, simulation artifacts, such as pop-up conflicts between newly introduced aircraft and existing aircraft, can cause $t_c < t_l$. Because the frequency of such artifacts is very much dependent on the design of the simulations themselves, and not by any naturally occurring interactions between aircraft, they are difficult to predict. Therefore, for the purposes of this derivation, t_c is considered to be a known input parameter. For the conditions studied here, t_c was found to be between 75-90% of t_l, depending on the value of t_l.

E. Step 3: Local Conflict Count Per Unit Distance Without CR

While the previous steps of the CAMDA framework have considered conflict counts for all traffic in the airspace (global), this step focuses on determining conflict counts, and conflict counts per unit distance flown, for a *single aircraft* without CR (local). These models are needed to bridge the CR OFF and CR ON parts of the CAMDA framework in subsequent steps.

Consider first the number of conflicts encountered by a single aircraft without CR, $C_{1,nr}$. This can be calculated by dividing $C_{total,nr}$ by the total number of aircraft in the airspace during the analysis time interval T without CR, $N_{total,nr}$:

$$C_{1,nr} = \frac{C_{total,nr}}{N_{total,nr}} \tag{9}$$

Subsequently, the number of conflicts per unit distance for a single flight, $C'_{1,nr}$, can be computed by dividing (9) by the average flight distance in the airspace volume of interest without CR, D_{nr}:

$$C'_{1,nr} = \frac{\Delta C_{1,nr}}{\Delta D_{nr}} = \frac{C_{total,nr}}{N_{total,nr}D_{nr}} \tag{10}$$

Note that the CAMDA method considers D_{nr} to be a known input parameter. To express $C'_{1,nr}$ as a function of ρ, a model for $N_{total,nr}$ as a function of ρ is needed. This can be derived as follows; to maintain a constant density of one aircraft in an airspace, the aircraft replacement rate would have to be V/D_{nr}. Likewise, to maintain a density of $N_{inst,nr}$ aircraft, the replacement rate would have to be $N_{inst,nr} \cdot V/D_{nr}$. Correspondingly, the total number of aircraft introduced during an analysis interval of length T would be $T \cdot N_{inst,nr} \cdot V/D_{nr}$. By using (7), and the logic described here, $N_{total,nr}$ can be formulated as:

$$N_{total,nr} = \frac{TVN_{inst,nr}}{D_{nr}} + N_{inst,nr} = \rho A\left(\frac{TV}{D_{nr}} + 1\right) \tag{11}$$

The first term on the right hand side of (11) is the number of aircraft that started their flights during the analysis time interval, while the second term is the number of aircraft that were already present in the airspace at the start of the analysis time. Substitution of (8) and (11) into (10) yields:

$$C'_{1,nr} = \frac{pTA\rho}{2t_c\left(TV + D_{nr}\right)} \tag{12}$$

F. Step 4: Local Conflict Count Per Unit Distance With CR

While the last three derivation steps considered the case *without CR*, the following three steps focus on conflict modeling *with CR*. Modeling the case with CR begins by developing an expression for the local conflict count per unit distance with CR, $C'_{1,wr}$, i.e., the 'with CR' counterpart of the previous step.

To model $C'_{1,wr}$, consider the motion of traffic within a decentralized system. In such a system, it is possible that there are no preferred directions, or because of a popular destination(s), there can be one or more preferred directions. Regardless of the type of heading distribution, CR maneuvers by a single aircraft, or by multiple aircraft in different parts of the airspace, are unlikely to affect the shape of the overall heading distribution of the total airspace. Because this logic can also be applied to all other traffic scenario distributions, such the altitude and spatial distribution of traffic, Jardin assumes that the number of conflicts *per unit distance* does not vary substantially with and without CR [10]. As described in section. II-B, this implies that the number of primary conflicts does not depend on CR. More formally, the first assumption used by CAMDA can be stated as:

CAMDA Assumption 1:

$$C'_{1,wr} \approx C'_{1,nr} \approx \frac{pTA\rho}{2t_c\left(TV + D_{nr}\right)} \tag{13}$$

As stated above, this assumption was used by Jardin, but it was not verified [10]. The results section of this paper, on the other hand, will specifically investigate the validity of

this assumption, and its effect on the final CAMDA capacity assessment, see section V-A.

G. Step 5: Total Conflict Count With CR

As stated before, to compute the DEP, it is necessary to derive a model of the total number of conflicts in an airspace with CR, $C_{total,wr}$. This can be computed by first considering the average number of conflicts for a single aircraft with CR, $C_{1,wr}$, which can in turn be expressed as the product of the average flight distance with CR, D_{wr}, and the local conflict count per unit distance with CR, $C'_{1,wr}$:

$$C_{1,wr} = D_{wr} C'_{1,wr} \tag{14}$$

Although $C'_{1,wr}$ was assumed to be not affected by CR, see (13), this can not be assumed for D_{wr}. This is because CR maneuvers cause aircraft to deviate from their nominal paths, and these deviations increase the total distance flown relative to the case without CR. Therefore, D_{wr} can be expressed as:

$$D_{wr} = D_{nr} + D_{cdr}\ C_{1,wr} \tag{15}$$

The above equation states that the distance flown by an aircraft with CR increases linearly with the number of conflicts detected. Here, the 'extra' distance flown as result of each conflict resolution maneuver, including the extra distance flown by an aircraft to recover its pre-conflict destination, is denoted as D_{cdr}. This parameter is affected by the type of CR algorithm used, and also by the occurrence of conflict chain reactions. As such, D_{cdr} is the sole empirical parameter of the CAMDA method, and therefore its value needs to be determined from simulation. Substituting (15) into (14) leads to:

$$C_{1,wr} = \frac{D_{nr} C'_{1,wr}}{1 - D_{cdr} C'_{1,wr}} \tag{16}$$

The above equation can be written as a function of ρ by substituting (13) into (16):

$$C_{1,wr} = \frac{pTD_{nr}A\rho}{2t_c\left(TV + D_{nr}\right) - pD_{cdr}TA\rho} \tag{17}$$

The total number of conflicts with CR, $C_{total,wr}$ can now be computed as the product between $C_{1,wr}$ and the total number of aircraft during the analysis time interval with CR, $N_{total,wr}$:

$$C_{total,wr} = C_{1,wr} N_{total,wr} \tag{18}$$

To formulate $N_{total,wr}$ as a function of ρ, the following assumption is made; although CR is expected to increase ρ due to longer flights, CR is also expected to increase the average distance flown by a proportional amount. Thus, the total number of aircraft during the analysis time interval is assumed to be similar with and without CR, as can be seen when this logic is applied to (11). More formally, the second assumption used by the CAMDA framework can be stated as:

CAMDA Assumption 2:

$$N_{total_{wr}} \approx N_{total_{nr}} \approx \rho A \left(\frac{TV}{D_{nr}} + 1\right) \tag{19}$$

The validity of this assumption is also tested in this work. A final expression for $C_{total,wr}$ as a function of ρ can be derived by substituting (17) and (19) into (18):

$$C_{total,wr} = \frac{pTA^2\rho^2\left(TV + D_{nr}\right)}{2t_c\left(TV + D_{nr}\right) - pD_{cdr}TA\rho} \tag{20}$$

H. Step 6: Modeling Capacity Using the DEP

The final step of the CAMDA framework uses the models developed above for $C_{total,nr}$ and $C_{total,wr}$ to express the DEP as a function of ρ. This allows the CAMDA capacity definition to be applied, enabling the calculation of the maximum theoretical capacity of a given airspace design, ρ_{max}. Substitution of (8) and (20) into (1) gives:

$$DEP = \frac{2t_c\left(TV + D_{nr}\right)}{2t_c\left(TV + D_{nr}\right) - pD_{cdr}TA\rho} - 1 \tag{21}$$

To apply the CAMDA capacity definition, it is useful to collect together all terms in the above equation that are *not* a function of ρ. To this end, λ and β are defined as:

$$\lambda = 2t_c\left(TV + D_{nr}\right) \tag{22a}$$

$$\beta = \frac{1}{pD_{cdr}TA} \tag{22b}$$

Using (22), (21) can be rewritten as:

$$DEP = \frac{\rho}{\lambda\beta - \rho} \tag{23}$$

The CAMDA capacity definition, given by (2), can now be evaluated. This involves determining the density at which the rate of change of the DEP with ρ equals infinity:

$$\left.\frac{dDEP}{d\rho}\right|_{\rho\to\rho_{max}} = \frac{\lambda\beta}{\left(\lambda\beta - \rho_{max}\right)^2} = \infty \tag{24}$$

Based on (24), it can be seen that the rate of change of the DEP with density equals infinity if, and only if, $\lambda\beta - \rho_{max} = 0$. Therefore, an infinite number of secondary conflicts is triggered per primary conflict when ρ_{max} is equal to $\lambda\beta$. Using (22):

$$\rho_{max} = \lambda\beta = \frac{2t_c\left(TV + D_{nr}\right)}{pD_{cdr}TA} \tag{25}$$

This equation shows that ρ_{max} is directly proportional to the ground speed of aircraft, V, and inversely proportional to the expected relative velocity between aircraft via the conflict probability p, see (4). Unsurprisingly, the above equation also states that ρ_{max} is dependent on the extra distance flown per conflict due to CD&R, D_{cdr}, i.e., the empirical parameter of the CAMDA method. Therefore, a value for ρ_{max} can be determined by fitting simulation logged DEP data to (23) in a least-squares sense. Thus, even though all parameters used by CAMDA have a physical meaning and take into account CD and CR, it is regarded as a *semi-empirical* method.

IV. Fast-Time Simulation Design

To demonstrate the utility of the CAMDA method, as well as to study the effects of CD parameters, CR dimension, and the speed distribution aircraft on airspace capacity, fast-time simulation experiments were performed for a decentralized direct routing en-route airspace concept. This section describes the design of these experiments.

A. Simulation Development

1) Simulation Platform

The BlueSky open-source ATM simulator [14], developed at TU Delft, was used as the simulation platform in this research.

2) Airborne Self-Separation Automation

As stated before, state-based CD was used in this study, see section III-C. It should be noted that CD was performed assuming perfect knowledge of aircraft states. This is in line with the findings of a recent study that concluded that ADS-B characteristics have little effect on the performance of state-based CD [15].

Once conflicts occurred, the Modified Voltage Potential (MVP) algorithm was used for CR. MVP works similar to the repulsion that occurs between similarly charged particles to resolve conflicts between aircraft in a pairwise fashion, resulting in implicit cooperative resolution strategies. This implies that all conflicting aircraft shared the task of avoiding intrusions using equal, but opposite, resolution maneuvers. It should be noted that MVP uses minimum-path deviation resolutions, and it was used for cases where CR was limited to either the

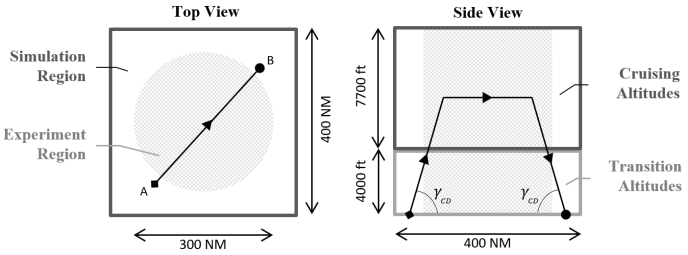

Fig. 5. Top and side views of the simulation's physical environment

horizontal or the vertical dimension. For a full description of the MVP algorithm, the reader is referred to [2], [16].

After CR, aircraft flew directly to their pre-conflict destinations in the horizontal direction, and recovered their pre-conflict altitudes in the vertical direction. This matches the functionality of most modern Flight Management Systems (FMS).

B. Traffic Scenarios

1) Testing Region and Flight Profiles

A large three-dimensional en-route sector was used as the physical environment for traffic simulations, see Fig. 5. Because no traffic was simulated outside the simulated sector, aircraft near the edges of the 'simulation region' are unlikely to get into conflicts. To solve this issue, a smaller cylindrical 'experiment region' was defined in the center of the 'simulation region'. The resulting gap between the experiment and simulation regions ensures that aircraft within the experiment region are surrounded by traffic in all directions. Correspondingly, only aircraft within the experiment region, and only conflicts with closest points of approach within the experiment region, were used to assess the accuracy of the CAMDA models.

Fig. 5 also shows the horizontal and vertical flight profiles of an example flight. Because the simulations consider a direct-routing airspace design, aircraft use direct-horizontal routes. Aircraft altitudes were selected to be linearly proportional to their flight distances. Since traffic scenarios with a uniform distribution of flight distances were used, this method of altitude selection resulted in a uniform distribution of aircraft cruising altitudes.

2) Scenario Generation

Ten traffic demand scenarios of increasing density, ranging between 8-80 aircraft per 10,000 NM^2 in the experiment region, were used for all three experiments. Note that this is more than twice the maximum traffic density of 32 aircraft per 10,000 NM^2 in the upper airspace (>18,000 ft) over the Netherlands in 2017 (computed using logged ADS-B data). Additionally, all traffic scenarios had uniform heading, altitude and spatial distributions. The speed distribution of aircraft varied between the three experiments, see section IV-C.

Traffic scenarios were generated with a duration of 2.5 hrs, consisting of a 1 hr traffic volume buildup period, a 1 hr logging period, and 0.5 hr wind-down period. Traffic density was held constant at the required level during the logging and wind-down periods. It should be noted that all scenarios were generated off line prior to the simulations so that all independent variables could be subjected to the same initial conditions.

C. Independent Variables

1) Conflict Detection Experiment

The goal of the first experiment was to investigate the effect of conflict detection parameters, namely horizontal and vertical separation requirements, and look-ahead time, on airspace capacity. Using different combinations of these three variables, three experiment conditions have been defined, see Table I. Experiments were performed for all ten traffic densities, ranging between 8-80 aircraft per 10,000 NM^2, using ten random initializations for each traffic density, and using an equal ground speed of 400 kts for all aircraft. Furthermore, to calculate the DEP from simulation data, scenarios were repeated with and without CR. In this experiment conflict resolutions were limited to the horizontal direction. This experiment resulted in a total of 600 runs, involving over 850,000 flights.

TABLE I
CONDITIONS OF CONFLICT DETECTION (CD) EXPERIMENT

Condition Name	S_h [NM]	S_v [ft]	t_l [mins]
Baseline	2.5	500	5.0
Double Separation	5.0	1000	5.0
Double Separation + Half Look Ahead	5.0	1000	2.5

2) Conflict Resolution Experiment

The second experiment focused on the effect of conflict resolution dimension on airspace capacity. Therefore, simulations were performed for ten traffic densities using the baseline CD setting for cases where conflict resolution was a) OFF, b) limited to the horizontal direction (combined heading and ground speed resolutions), and c) limited to the vertical direction (vertical speed resolutions). For this purpose, the MVP CR algorithm was used, resulting in a cooperative resolution maneuvers, see section IV-A2. Once again ten repetitions were performed at each traffic density, and all aircraft flew with an equal ground speed of 400 kts. This simulation resulted in a total of 300 simulation runs, using over 425,000 flights.

3) Ground Speed Experiment

The final experiment considered the effect of the equal speed assumption that was made during the derivation of the CAMDA models. Therefore in this experiment, simulations were performed for all ten traffic densities and for cases where the speed distribution of aircraft was a) equal at 400 kts, b) normally distributed with a mean of 400 kts and a standard deviation of 16.7 kts, and c) uniformly distributed between 350-450 kts. Once again, each traffic density was repeated 10 times, and scenarios were repeated with and without CR to calculate the DEP from simulation data. In this experiment resolutions were limited to the horizontal direction. This experiment resulted in a total of 600 runs, involving over 850,000 flights.

D. Dependent Variables

In addition to studying the effects of CD parameters, CR dimension and the speed distribution of aircraft on airspace capacity, data collected from the experiments was also used to assess the accuracy of the CAMDA modeling approach. The specific approach used to measure accuracy varied between the analytical and semi-empirical components of the CAMDA framework. The appropriate methods are discussed with the corresponding results in the following section.

V. RESULTS AND DISCUSSION

In this section, the results of the three simulation experiments are presented and discussed. As stated before, the results apply for a decentralized direct-routing en-route airspace design.

A. Conflict Detection Experiment

The goal of the Conflict Detection (CD) experiment is to study the effect of horizontal and vertical separation requirements, and look-ahead time, on the capacity of the airspace, see Table I. Data gathered from this experiment is also used to analyze the accuracy of all CAMDA sub-models. The following paragraphs discuss the results of the analytical and the semi-empirical components of the CAMDA framework separately.

1) Analytical Model Components

Figure 6 displays the simulation results for the analytical components of the CAMDA method. In this figure, the scatter points represent the raw data collected from the simulations, and the solid lines represent the model predictions for each CAMDA component. To assess the accuracy of analytical models, a model accuracy parameter, k, is introduced, as illustrated below for a generic case:

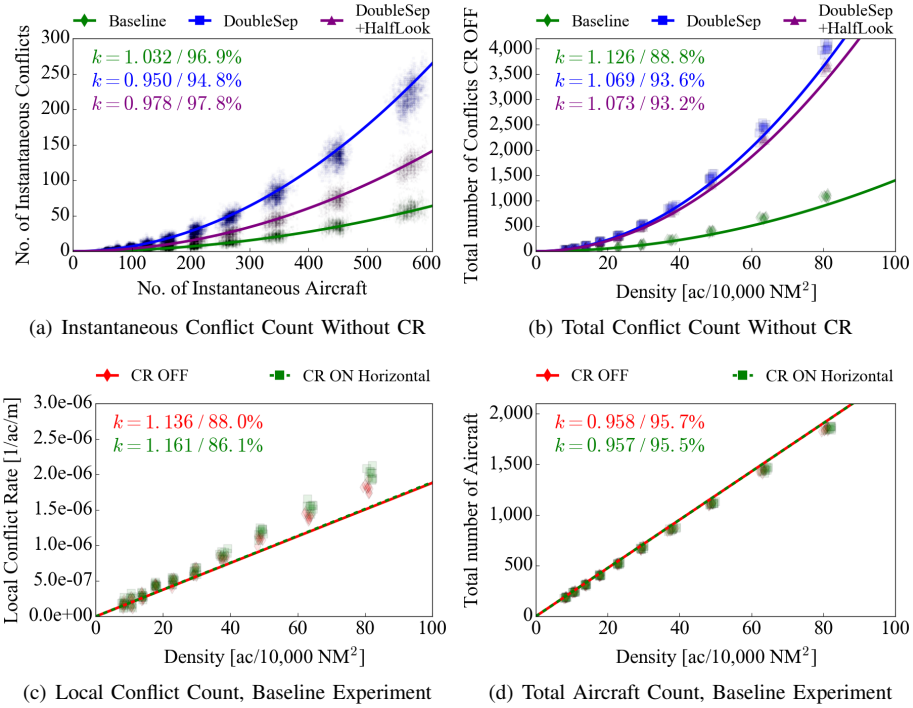

(a) Instantaneous Conflict Count Without CR

(b) Total Conflict Count Without CR

(c) Local Conflict Count, Baseline Experiment

(d) Total Aircraft Count, Baseline Experiment

Fig. 6. Simulation data (scatter) and model predictions (lines) for analytical components of the CAMDA framework, Conflict Detection (CD) experiment

$$\text{Simulation Measurement} = \text{Analytical Model} \times k$$

Here it can be seen that k acts as a constant scaling parameter to the analytical models. Its value is determined by fitting the models to the simulation data in a least-square sense. A value of k close to 1 indicates high model accuracy, while $k < 1$ and $k > 1$ indicates model over- and under-estimation of simulation data, respectively. Model accuracy is also computed as a percentage by comparing the fitted k to a reference value of 1.

Instantaneous Conflict Count Without CR, $C_{inst,nr}$

The results for $C_{inst,nr}$ are displayed in Fig. 6(a). The figure shows that the analytical model, given by (3), is able to closely predict both the shape and the magnitude of the simulation data very closely for all densities, and for all CD conditions. This high accuracy is also reflected by k values that are very close to 1.0. On comparing the three curves in Fig. 6(a), it can be seen that separation requirement has a greater effect on $C_{inst,nr}$ than look-ahead time.

Total Conflict Count Without CR, $C_{total,nr}$

Figure 6(b) shows the results for the second model of the CAMDA framework, namely $C_{total,nr}$. In contrast to $C_{inst,nr}$, this figures shows that look-ahead time does not significantly affect $C_{total,nr}$. This can be explained by the fact that the model for $C_{total,nr}$, given by (8), contains look-ahead time, t_l, in the numerator (via the conflict probability, p), and conflict duration, t_c, in the denominator. Since these two parameters have similar values, the effect of t_l on $C_{total,nr}$ is, therefore, almost 'canceled-out'.

Although the model curves in Fig. 6(b) closely follow the trend between $C_{total,nr}$ and traffic density, it is clear that equation (8) slightly underestimates $C_{total,nr}$. This is also indicated by $k > 1$ for all conditions. Moreover, the model accuracies for $C_{total,nr}$ are lower than for $C_{inst,nr}$. This is because CAMDA uses a sequential framework, and therefore any modeling errors will accumulate further down the framework. Nonetheless, model accuracy is still approximately 90% for all cases. This means that equation (8) still provides a good understanding of the relationships between the factors that affect $C_{total,nr}$.

Local Conflict Count Per Unit Distance, C'_1

The results for C'_1 with and without CR are pictured in Fig. 6(c). Note that due to limited space, the figure only displays the results for the 'baseline' condition; the results of the other conditions are similar. Moreover, the baseline condition led to the *lowest* model accuracy, similar to $C_{total,nr}$.

An important assumption made by the CAMDA method to bridge the cases with and without CR is that $C'_{1,wr} \approx C'_{1,nr}$, see (13). Analysis of Fig. 6(c) shows that this assumption is true up to a density of approximately 40 aircraft per 10,000 NM^2. But beyond this density, the simulation data indicates $C'_{1,wr} > C'_{1,nr}$. Furthermore, the difference between the model predictions and the simulation results appears to increase beyond this density. It is hypothesized that the larger number of conflict chain reactions that occur at higher densities leads to a break-down of this assumption; for instance, if such conflict chains are concentrated in one or more parts of the airspace, then it is logical that the local conflict count per unit distance with CR would increase relative to the case without CR case.

Regardless, Fig. 6(c) indicates that the first assumption made by the CAMDA framework, that $C'_{1,wr} \approx C'_{1,nr}$, is only valid for densities that are comparable to the peak densities for todays operations (32 aircraft per 10,000 NM^2). For densities that are approximately three times greater than today, this assumption does not hold in a purely mathematical sense. However, because the absolute difference between model and simulation at the highest simulated density is less than 5e-7 conflicts per aircraft per meter, the violation of this assumption is not likely to affect the final CAMDA capacity estimate; at this level of difference, an aircraft would have to fly more than an additional 1000 NM in the simulation for it to encounter just one additional conflict relative to the model prediction for the baseline condition. This conclusion is further exemplified model accuracies which are greater than 85%.

Total Aircraft Count, N_{total}

The CAMDA framework assumes that $N_{total,wr} \approx N_{total,nr}$. To validate this assumption, results for N_{total} for the 'baseline' condition are displayed in Fig. 6(d). The results for the other two conditions are similar, but are not shown because the corresponding model, given by (19), is independent of CD parameters. This figure shows that the model for N_{total} closely matches the simulation data for the cases with and without CR. The high accuracy is further emphasized by k values that are very close to 1. Therefore it can be concluded that the

second assumption used by CAMDA is valid for all considered densities.

2) Semi-Empirical Model Components

The last two models of the CAMDA framework, namely $C_{total,wr}$ and the DEP, are influenced by D_{cdr}. This parameter describes the extra distance flown by an aircraft to resolve each detected conflict. Because D_{cdr} is affected by conflict chain reactions, its value can only be determined by fitting the model for $C_{total,wr}$, or the model for the DEP, to the simulation data in a least-squares sense. Since these two models are semi-empirical, it is not possible to measure model accuracy using the procedure outlined earlier for the analytical components of the CAMDA framework.

Instead, the accuracy of semi-empirical models can be determined by considering two aspects. The first aspect is *qualitative*, and it considers the ability of a model to predict the shape of the relationship between traffic density and the airspace state of interest, in this case $C_{total,wr}$ and the DEP. This aspect can be studied visually by checking whether the shape of the fitted model curve follows the trends displayed by the raw simulation data.

The second aspect aims to *quantify* the accuracy of the fitting process. To this end, the available simulation data is split into two datasets of equal size, known as the 'training' and the 'validation' datasets. Only the training dataset is used to determine the semi-empirical parameters. Subsequently, the Root Mean Square (RMS) error between model predictions and the empirical data is computed for both training and validation datasets. If the RMS error for the training data set is small, then the fitting accuracy is considered to be high. If the RMS errors for the training and validation datasets are comparable, then the model fitting process was not significantly affected by simulation artifacts and noise, i.e, over-fitting was limited.

Total Conflict Count With CR, $C_{total,wr}$

Figure 7(a) shows the results for $C_{total,wr}$. This figure shows that separation requirement has a large effect, while look-ahead time has a minimal effect, on $C_{total,wr}$, a trend also noted above for $C_{total,nr}$. Furthermore, as the fitted model curves closely approximate the shape and magnitude of the simulation data, it can be concluded that structure of equation (20) well represents $C_{total,wr}$.

To quantify the accuracy of the models fits for $C_{total,wr}$, Fig. 7(b) displays the RMS errors for the training and validation datasets. This figure shows that the errors are low for the 'baseline' and for the 'double separation + half look-ahead' conditions. However, the RMS errors for the 'double separation' condition is relatively high. On close inspection of Fig. 7(a), it can be seen that the fitting error for the double separation condition arises mainly at the highest traffic density. It is important to consider the magnitude of this fitting error in view of the number of conflicts that occurred during the simulation at this density; an RMS error of 188 conflicts for the validation dataset of the double separation condition corresponds to an error of only 3% relative to the actual number of conflicts logged at this density. Therefore, while the RMS errors are larger for the double separation condition in a relative sense, they are quite low in the absolute sense. For this reason, the accuracy of the model fits for all CD conditions can be considered to be high.

Domino Effect Parameter (DEP) and Airspace Capacity, ρ_{max}

The results for the DEP, the final and most important component of the CAMDA framework, are pictured in Fig. 7(c). As expected, the figure shows that the DEP, which considers the occurrence and propagation of conflict chain reactions, increases with traffic density for all experiment conditions. Although the simulation results for low traffic densities are very noisy, the figure still shows that the model for the DEP, given by (23), is able to well characterize the shape and magnitude of the logged simulation data. The high accuracy of the model fitting process is further indicated by the low RMS errors found for both training and validation datasets, see 7(d).

Because the DEP model matches well with the simulation data, it is possible to apply the CAMDA capacity definition, given by (2), to analyze the effect of CD parameters on the maximum theoretical capacity of the direct-routing airspace concept considered here. From a graphical point of view, this entails determining the traffic density corresponding to the vertical asymptote of the model fitted curves.

Using this procedure, ρ_{max} for all three CD conditions is computed, see Fig. 7(c). As for many of the other metrics, this figure shows that separation requirement has a significantly greater effect on airspace capacity than look-ahead time. This trend can be explained by considering equation (25). This equation states that CD parameters affect ρ_{max} via the conflict probability, p, which is in turn described by (4). The later equation states that a doubling of look-ahead time, for instance, would lead to a doubling of p, while a doubling of the horizontal and vertical separation requirements would lead to a quadrupling of p. This effect of CD parameters on p explains the relative capacity differences between the three CD conditions considered here. This example also illustrates the utility of the CAMDA method; even though CAMDA is semi-empirical, because all underlying models and parameters are derived with a physical interpretation, the effect of a number of airspace parameters can be directly understood from the structure of the models themselves.

B. Conflict Resolution Experiment

The second experiment investigated the effect of conflict resolution dimension on airspace capacity. To this end, simulations were repeated for the cases where conflict resolution was a) limited to the horizontal direction and b) limited to the vertical direction.

The DEP and capacity results for the CR experiment are shown in Fig. 8. Here it can be seen that the airspace becomes more unstable when vertical conflict resolutions are used. In fact, limiting CR in the vertical direction decreases airspace capacity by a factor of three.

Although the horizontal separation requirement is 30 times larger than the vertical separation minima for the settings used in this experiment, this unusual result can be explained by considering the horizontal and vertical density distributions of aircraft in the airspace. In en-route airspace, aircraft tend to be more closely packed in the vertical direction than in the horizontal plane. For example, most long-distance flights cruise between FL300-FL400, whereas aircraft can be separated laterally by many nautical miles. As a result of the closer packing of aircraft along the vertical direction, vertical conflict resolution maneuvers are more likely to trigger new conflicts, and therefore, more like to cause conflict chain reactions. Consequently, vertical resolutions reduce the maximum theoretical capacity of the airspace.

C. Ground Speed Experiment

To reduce the complexity of the derivation process, the models described in this paper assume equal grounds speeds for all aircraft in the airspace. To study the effect of this assumption on the accuracy of the CAMDA method, simulations were performed for the cases where aircraft speeds were a) equal, b) normally distributed and c) uniformly distributed.

The DEP and capacity results for the ground speed experiment are displayed in Fig. 9. This figure shows no substantial differences in the DEP for the three speed distributions tested. Moreover, the CAMDA capacity estimate for the normal and uniform distributions are within 5% of the capacity estimated for the case where all aircraft flew with equal ground speeds. This can be explained by the fact that the mean speed of all considered distributions was the same. This result suggests that accurate capacity estimates can be computed using the CAMDA approach as the long as the average speed of all aircraft in the airspace is known, regardless of the shape of the speed distribution of aircraft.

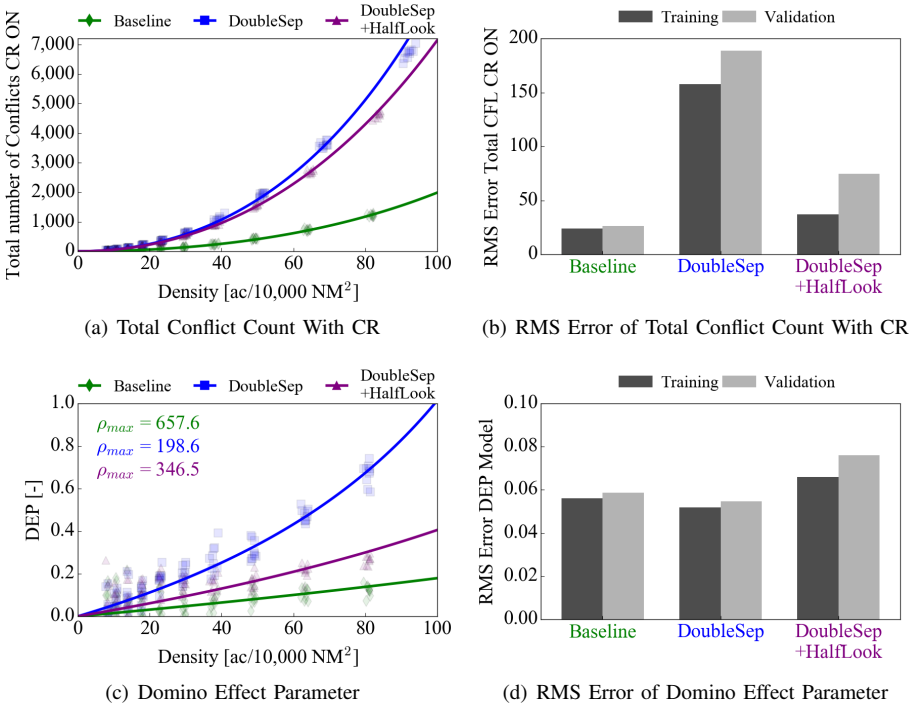

(a) Total Conflict Count With CR

(b) RMS Error of Total Conflict Count With CR

(c) Domino Effect Parameter

(d) RMS Error of Domino Effect Parameter

Fig. 7. Simulation data (scatter) and model fits (lines) for semi-empirical components of the CAMDA framework, Conflict Detection (CD) experiment

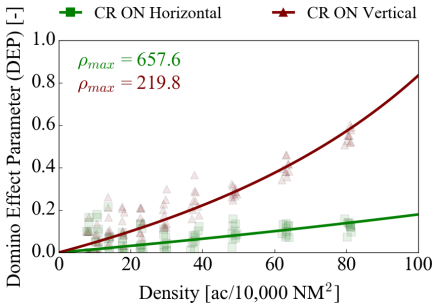

Fig. 8. Domino effect parameter and airspace capacity results for the Conflict Resolution (CR) experiment

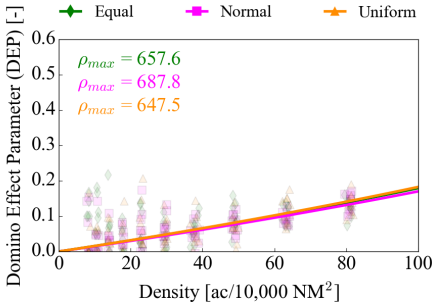

Fig. 9. Domino effect parameter and airspace capacity results for the ground speed experiment

VI. Conclusions

This paper presented the derivation of the Capacity Assessment Method for Decentralized ATC (CAMDA). CAMDA was demonstrated in this work using three-dimensional simulations of a decentralized direct-routing en-route airspace concept. The following conclusions can be drawn:

- CAMDA defines the capacity of the airspace as the density at which the Domino Effect Parameter (DEP), a measure of airspace stability, approaches infinity. At this density, all aircraft in the airspace exist in a persistent state of conflict due to uncontrollable conflict chain reactions.
- Fast-time simulation results showed that the underlying CAMDA models can accurately predict the occurrence of conflict chain reactions, enabling capacity estimations using relatively non-intensive low-density traffic scenarios.
- It was found that changes to traffic separation requirements had a greater impact on airspace capacity than changes to the conflict detection look-ahead time. This is because separation requirements have a larger effect on the average conflict probability between aircraft.
- Because aircraft tend to be more closely packed in the vertical direction than in the horizontal direction, cooperative vertical conflict resolution maneuvers cause a larger number of conflict chain reactions, decreasing airspace capacity relative to cooperative horizontal conflict resolution maneuvers.
- Using different speed distributions for aircraft did not significantly affect the capacity of the direct-routing airspace concept considered in this work. This indicates that accurate capacity estimates can be computed using CAMDA if the average speed of all aircraft is known.
- To further increase CAMDA accuracy, it is recommended to investigate methods to relax modeling assumptions, particularly an assumption concerning the local conflict count per unit distance with conflict resolution.
- CAMDA relies on the conflict probability between aircraft to compute the maximum theoretical capacity for decentralized ATC. The conflict probability modeling component of CAMDA could be used as a starting point to develop similar methods for current-day operations. This will be the topic of future research.

As a final note, it is important to realize that CAMDA determines the *absolute* maximum *theoretical capacity* of an airspace design. In practice, however, society will not recognize an asymptotic limit of airspace stability as an acceptable definition of airspace capacity. Moreover, airline economics, which is primarily focused on improving efficiency, and stochastic effects, such as weather, affect the *practical capacity* of the airspace. Nevertheless, the theoretical capacity limit determined by CAMDA can be used as a fair and objective metric for comparing different decentralized airspace designs, and/or CD&R algorithms.

Acknowledgments

The authors would like to thank Junzi Sun, PhD candidate, TU Delft, for calculating the maximum traffic density over the Netherlands in 2017 using logged ADS-B data. This research would not been possible without the efforts of the open-source community that continually contributes to the development of the BlueSky ATM simulator.

BlueSky can be downloaded from https://github.com/ProfHoekstra/bluesky.

REFERENCES

[1] Performance Review Commission, "Eurocontrol Performance Review Report 2016," Eurocontrol, Tech. Rep. PRR2016, 2016.

[2] J. M. Hoekstra, R. N. H. W. van Gent, and R. C. J. Ruigrok, "Designing for safety: the free flight air traffic management concept," *Reliability Engineering & System Safety*, vol. 75, no. 2, pp. 215–232, Feb. 2002.

[3] J. M. Hoekstra, R. C. J. Ruigrok, and R. N. H. W. van Gent, "Free Flight in a Crowded Airspace?" in *Proceedings of the 3rd USA/Europe Air Traffic Management R&D Seminar*, Naples, Jun. 2000.

[4] M. Ballin, J. Hoekstra, D. Wing, and G. Lohr, "NASA Langley and NLR Research of Distributed Air/Ground Traffic Management," in *AIAA Aircraft Technology, Integration, and Operations (ATIO) Conference, AIAA-2002-5826*, 2002.

[5] J. K. Kuchar and L. C. Yang, "A Review of Conflict Detection and Resolution Modeling Methods," *IEEE Transactions on Intelligent Transportation Systems*, vol. 1, pp. 179–189, 2000.

[6] E. Sunil, J. Ellerbroek, J. Hoekstra, A. Vidosavljevic, M. Arntzen, F. Bussink, and D. Nieuwenhuisen, "Analysis of Airspace Structure and Capacity for Decentralized Separation Using Fast-Time Simulations," *Journal of Guidance, Control, and Dynamics*, vol. 40, no. 1, pp. 38–51, 2017.

[7] F. Maracich, "Flying free flight: pilot perspective and system integration requirement," *IEEE Aerospace and Electronic Systems Magazine*, vol. 21, no. 7, pp. 3–7, Jul. 2006.

[8] K. Bilimoria, K. Sheth, H. Lee, and S. Grabbe, "Performance evaluation of airborne separation assurance for free flight," in *AIAA Guidance, Navigation and Control Conference*, 2000.

[9] J. Krozel, M. Peters, and K. Bilimoria, "A decentralized control strategy for distributed air/ground traffic separation," in *AIAA Guidance, Navigation, and Control Conference and Exhibit*, 2000.

[10] M. R. Jardin, "Analytical Relationships Between Conflict Counts and Air-Traffic Density," *Journal of Guidance, Control, and Dynamics*, vol. 28, no. 6, pp. 1150–1156, 2005.

[11] Hoekstra, J., Maas, J., Tra, M., and Sunil, E., "How Do Layered Airspace Design Parameters Affect Airspace Capacity and Safety?" in *Proceedings of the 7th International Conference on Research in Air Transportation*, Jun. 2016.

[12] Sunil, E., Ellerbroek, J., Hoekstra, J.M., and Maas, J., "Three-Dimensional Conflict Count Models for Unstructured and Layered Airspace Designs," *submitted to Transportation Research Part C: Emerging Technologies*, Dec. 2017.

[13] Sunil, E., rarson, O., Ellerbroek, J., and Hoekstra, J.M., "Analyzing the Effect of Traffic Scenario Properties on Conflict Count Models," in *Submitted to International Conference on Research in Air Transportation (ICRAT '18)*, Jun. 2018.

[14] J. Hoekstra and J. Ellerbroek, "BlueSky ATC Simulator Project: an Open Data and Open Source Approach," in *Proceedings of the 7th International Conference on Research in Air Transportation*, Jun. 2016.

[15] T. Langejan, E. Sunil, J. Ellerbroek, and J. Hoekstra, "Effect of ADS-B Characteristics on Airborne Conflict Detection and Resolution," in *Proccedings of the 6th Sesar Innovation Days*, 2016.

[16] J. M. Hoekstra, "Designing for safety: the free flight air traffic management concept," PhD Dissertation, Delft University of Technology, Delft, Nov. 2001. [Online]. Available: http://resolver.tudelft.nl/uuid:d9f6078a-0961-403f-871e-cad365ee46a9